

# OBJECTIVE IMAGE QUALITY MEASURES BY PLANAR GLYPH REPRESENTATION

*C. Vertan*<sup>1,2</sup>, *A. Stoica*<sup>1,2</sup>, *C. Fernandez-Maloigne*<sup>2</sup>, *M. Ciuc*<sup>1</sup>

<sup>1</sup> LAPI, Bucharest Politehnica University, Romania

P.O. Box 35-57, Bucharest 35, Romania

phone: + 40 21 402 4683, fax + 40 21 402 4821, email: {cvertan, mciuc}@alpha.imag.pub.ro

<sup>2</sup> IRCOM-SIC, University of Poitiers, France

Bat. SP2MI, BP30179, 86962 FUTUROSCOPE Chasseneuil Cedex, France

phone: + 33 5 49496567, fax + 33 5 49496570, email{stoica,fernandez}@sic.sp2mi.univ-poitiers.fr

## ABSTRACT

The commonly used non-perceptual image quality measures are mainly derived from pixel-to-pixel differences and closely relate to the mean squared error. Recently, there has been an increased interest in the evaluation of neighborhood-based differences between images, that take into account the local (spatial) image context. This contribution proposes the use of such local context information for the evaluation of image quality or inter-image differences by the planar glyph representation of multivariate data and the induced geometric-inspired difference measures.

## 1. INTRODUCTION

Classically, the difference between images is measured by mean squared error-type differences and their normalized versions, such as the signal-to-noise ratio (SNR). This type of objective measures account only for pixel-to-pixel differences and not for the local (spatial) image context and does not comply to the human visual system characteristics. Several image difference (and image quality) measures have been introduced in order to accommodate the two (related) problems of the local pixel context and correlation to the perceptual observations [5], [4].

One of the most recently introduced image quality measures is the image quality index (Q-index), introduced by Wang and Bovik [11] as:

$$Q = \frac{4\sigma_{I_1 I_2} \overline{I_1 I_2}}{(\sigma_{I_1}^2 + \sigma_{I_2}^2)(\overline{I_1}^2 + \overline{I_2}^2)} \quad (1)$$

In the equation above, the quality index  $Q$  measures the distance between images  $I_1$  and  $I_2$ , based on the local means ( $\overline{I_1}$ ,  $\overline{I_2}$ ), variances ( $\sigma_{I_1}^2$ ,  $\sigma_{I_2}^2$ ) and covariance ( $\sigma_{I_1 I_2}$ ) of the images to be compared. As described by the authors, this index models various distortions as a combination of three factors: loss of correlation, distortion of luminance and distortion of contrast. The statistical mean, correlation and variance are measured locally, in a neighborhood of each pixel of the two images  $I_1$  and  $I_2$  that are to be compared. We shall use this Q-index as further comparison basis, since it uses local measures and is shown to be well correlated to the subjective judgements [11].

The remainder of the paper is organized as follows: section 2 explains the glyph representation of multivariate data,

section 3 introduces the proposed distances derived from the glyph representation and section 4 presents experimental results on image quality measurement and contour extraction. Finally, section 5 presents some conclusions of this work.

## 2. GLYPH REPRESENTATION OF MULTIVARIATE DATA

We propose to exploit a new approach, inspired by the reduced ordering principle of Barnett [2] that has also been used in multivariate data visualization [7]. The idea is to map the multivariate data to some familiar, two-dimensional objects, that can be grouped, compared, and plotted in a more suitable fashion for human perception. Examples of such mappings are the Chernoff faces [3], [7], the Andrews curves [1] and their possible extensions [9], the basic and modified parallel coordinates [7] and the star glyphs [7].

A star glyph associated to a  $p$ -dimensional ( $p > 2$ ) data vector is a polygon obtained by connecting  $p$  points in the two-dimensional plane. The points are taken along  $p$  origin-concurrent, equally-spaced axes that span the two-dimensional plane (obviously, the angle between every two successive axes is  $2\pi/p$ ). Each axis is associated to one component of the vector data, which is plotted according to its magnitude (see two examples in figure 1). For example, the star glyph that corresponds to  $p = 3$  (figure 1 a)) is a triangle and can be used for representing colors (three-dimensional vectors) in the two-dimensional plane. The same type of representation can accommodate data of higher dimensions, such as the vector formed with the values of pixels located in a fixed neighborhood of a given pixel.

In the following we shall focus on the use of a usual  $3 \times 3$  neighborhood. Let  $x^*$  be the value of the current pixel (the pixel located at the center of the neighborhood) and  $x_1$  to  $x_8$  the values of its 8 neighbors. The local relative context can be measured by the eight differences  $y_i = |x_i - x^*|$ ,  $i = 1, \dots, 8$ . The associated graphical representation is an octagonal glyph (see figure 1 b)).

## 3. A GEOMETRIC-BASED INTER-GLYPH DISTANCE

Intuitively, we may consider the similarity measure between vectors as the area of the intersection between the two associated glyphs. In order to construct a symmetrical and normalized measure, we will follow the approach used by Swain [8] in the definition of the distance between color histograms: the normalization has to be performed with respect to the

---

The authors acknowledge the support of the CNCSIS Grant AT13/2003

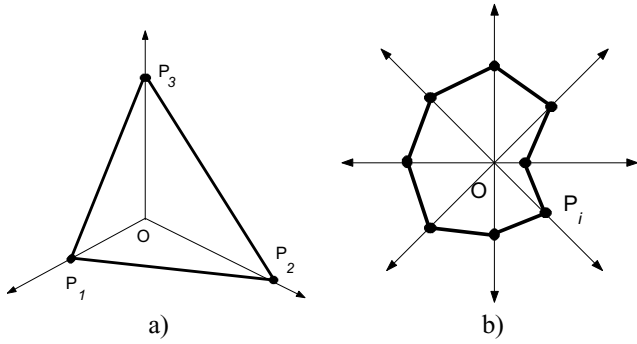


Figure 1: a) Star glyph associated to a three-component vector  $\mathbf{C} = (x_1, x_2, x_3)$  (a color, for instance). The angles between axes are  $2\pi/3 = 120^\circ$ ; the points  $P_i$  ( $P_1, P_2, P_3$ ) are placed on axes  $i$  at distance  $\|OP_i\| = x_i$ . The star glyph is the  $P_1P_2P_3$  polygon (thick black line). b) Star glyph associated to the eight-dimensional difference vector  $\{y_i\}$ ,  $i = 1, \dots, 8$  that represents the local context of a given pixel. The angles between axes are  $2\pi/8 = 45^\circ$ ; the points  $P_i$  are placed on axes  $i$  at distance  $\|OP_i\| = y_i$ . The star glyph is the octogon drawn with the thick black line.

maximum area of the two polygons. Thus, the similarity between vectors  $\mathbf{v}_1$  and  $\mathbf{v}_2$ , represented by their corresponding glyphs  $G_1$  and  $G_2$ , is:

$$\text{Sim}(G_1, G_2) = \frac{\text{Area}(G_1 \cap G_2)}{\max\{\text{Area}(G_1), \text{Area}(G_2)\}}. \quad (2)$$

The similarity defined in (2) can be transformed into a distance by:

$$d(G_1, G_2) = 1 - \text{Sim}(G_1, G_2). \quad (3)$$

Such an approach was previously used in [10] as a means to define an inter-color distance which was further used for distance-based color image filtering.

#### 4. IMAGE DIFFERENCE MEASURES AND USAGE

Let us consider the equally-sized,  $M \times N$  scalar (gray-scale) images  $\mathbf{I}_1$  and  $\mathbf{I}_2$ . The difference between the two images is evaluated on the basis of both the local context of each pixel (measured by the differences between the value of the central pixel and the values of its neighbors and represented by the octogonal glyph) and the value of that pixel itself (in a one-to-one comparison). Since the value of the current pixel is a more significant and relevant information than its local context, it is not directly mixed into the planar glyph representation. We shall rather imagine the geometrical model of a parallelepiped with the base given by the local context (the octogonal glyph) and the height equal to the value of the current pixel.

The distance between two pixels placed in images  $\mathbf{I}_1$  and  $\mathbf{I}_2$  at the same spatial location  $(m, n)$  and described by local contexts represented by the glyphs  $G_1$  and  $G_2$  reduces to the comparison of their associated parallelepipeds by a distance similar to (2) and (3):

$$d(\mathbf{I}_1(m, n), \mathbf{I}_2(m, n)) = 1 - \frac{\min\{\mathbf{I}_1(m, n), \mathbf{I}_2(m, n)\} * \text{Area}(G_1 \cap G_2)}{\max\{\mathbf{I}_1(m, n) * \text{Area}(G_1), \mathbf{I}_2(m, n) * \text{Area}(G_2)\}}. \quad (4)$$

The equation (4) can be explained as follows: the similarity between two parallelepipeds is the ratio of their common volume to the maximum of the two volumes. The distance is one minus the similarity.

The distance between the images  $\mathbf{I}_1$  and  $\mathbf{I}_2$  is the average distance between their pixels, computed according to (4):

$$d(\mathbf{I}_1, \mathbf{I}_2) = \frac{1}{MN} \sum_{m=1}^M \sum_{n=1}^N d(\mathbf{I}_1(m, n), \mathbf{I}_2(m, n)). \quad (5)$$

#### 4.1 Inter-image difference

There is a straightforward way to measure inter-image differences according to the method defined above, in order to establish a quality measure. For the given pair of images,  $\mathbf{I}_1$  and  $\mathbf{I}_2$ , where  $\mathbf{I}_1$  is the reference (original, undegraded) image and  $\mathbf{I}_2$  is the degraded (or transformed) image, the measure of quality is the inter-image distance, defined according to (5).



Figure 2: Peppers image degraded with additive Gaussian noise and 2% impulsive noise.

We tested the proposed quality measure for images degraded by Gaussian, additive white noise, blurring and JPEG compression, at five levels of degradation (Gaussian noise of variance 5, 10, 20, 30, 40; blurring by averaging within  $3 \times 3$ ,  $5 \times 5$ ,  $7 \times 7$ ,  $9 \times 9$  and  $11 \times 11$  neighborhoods; JPEG compression at quality factors of 90, 75, 60, 45 and 30).

As expected, the inter-image distance defined according to (5) is increasing with respect to the amount of image degradation, just as the classical mean squared error.

We performed also a correlation test of the inter-image differences with respect to the perceptual (subjective) grading of image distance, as judged by human observers. For the test images, 6 observers were asked to grade the measure of degradation of each of the tested images. The subjective grades were then linearly regressed onto the various objective distance measures used (proposed distance, MSE, Q index). Table 1 presents the absolute value of the correlation coefficients of the subjective and objective values for various degradation methods used. As it can be easily noticed, the perceptual grading is maximally correlated to the proposed distance measure.

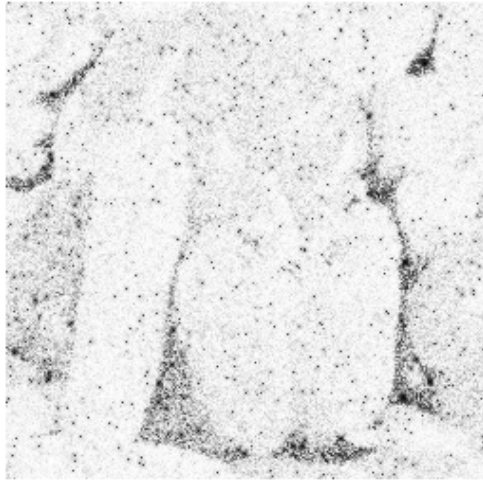


Figure 3: Pixel difference map for the degraded image from figure 2 computed according to (4). The most important differences are mapped into darker gray tones; it can be noticed that the white noise impulses superimposed on dark image areas are producing the biggest differences, as visually perceived by an observer.



Figure 4: Original Lena image.

Degradation \ Measure	SNR	Q	Glyph
Gaussian noise	-0.958	0.957	0.988
Blurring	-0.915	0.930	0.969
JPEG compression	-0.894	0.841	0.920

Table 1: Correlation coefficients between the average perceptual grading of image degradation and the tested objective image quality measures. The image quality measure based on the proposed planar glyph representation of the local image context is the most correlated with the subjective judgments.

#### 4.2 Contour extraction

Let us consider that the image  $I_2$  is a blurred version of the original image  $I_1$ . The differences between the two images

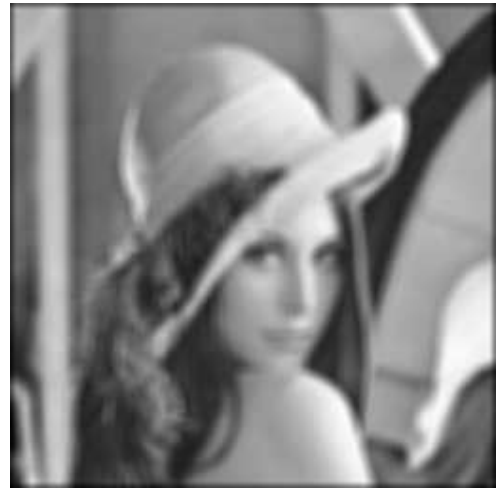


Figure 5: Heavily blurred version of original Lena image.



Figure 6: JPEG compressed version of Lena image (quality factor 50).

are located along the edges and details of the objects within [6]. Thus, the map of the inter-pixel differences, computed according to (4) is an edge intensity map that can be used for contour extraction.

The contour thickness and the contour sensitivity can be controlled by the amount of blurring applied to the original image. The following figures present some examples of edge intensity maps extracted from classical test gray-level images by the proposed method with various amounts of blurring.

## 5. CONCLUSIONS

This contribution proposed a new method for the evaluation of image quality or inter-image differences by the use of local context information. The values from each pixels neighborhood are mapped to a planar glyph representation (as primarily used in multivariate data representation and analysis). The comparison is performed at the neighborhood level by some geometric-inspired normalized difference measures,

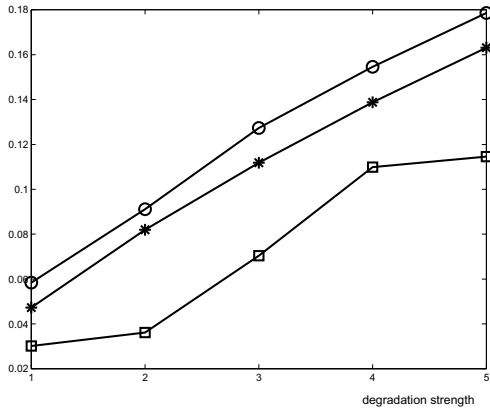


Figure 7: Plot of the proposed glyph-based image quality measure for the test images used with respect to the degradation strength: additive Gaussian noise (circle marks), blur (star marks) and JPEG compression (square marks).



Figure 8: Edge intensity map of the Lena test image computed according to the proposed method, using a blurring by 3 x 3 neighborhood averaging.

induced by the particular nature of the glyph representation.

We compared the proposed inter-image distance based on glyph representation with two classical image quality measures – the signal to noise ratio and the universal image quality index – for the correlation to the perceptual grading of three distortion types: blurring, JPEG compression and additive noise. The tests showed that the proposed measure is more correlated to the subjective judgement than its counterparts.

## REFERENCES

- [1] D. F. Andrews. Plots of high-dimensional data. *Biometrics*, 28:125–136, 1972.
- [2] V. Barnett. The ordering of multivariate data. *J. of Royal Stat. Soc. A*, 139(3):318–354, 1976.
- [3] H. Chernoff. The use of faces to represent points in



Figure 9: Edge intensity map of the Lena test image computed according to the proposed method, using a blurring by 5 x 5 neighborhood averaging.

k- dimensional space graphically. *J. of the American Statistical Association*, 68:125–136, 1973.

- [4] S. Daly. The visible differences predictor: An algorithm for the assessment of image fidelity. *Proceedings of SPIE*, 1616:2–15, 1992.
- [5] A. M. Eskicioglu, P.S. Fisher, and S. Chen. Image quality measures and their performance. *IEEE Transactions on Communications*, 43(12):2959–2965, 1995.
- [6] A.K. Jain. *Fundamentals of Digital Image Processing*. Prentice Hall Intl., Englewood Cliffs NJ, 1989.
- [7] W. J. Krzanowski. *Principles of Multivariate Analysis: A User's Perspective*. Clarendon Press, Oxford, 1993.
- [8] M. J. Swain and D. H. Ballard. Color indexing. *International Journal of Computer Vision*, 7(1):11–32, 1991.
- [9] C. Vertan, M. Ciuc, and V. Buzuloiu. Multichannel median filtering by wavelet series expansion. In *Proc. of the 6th International Workshop on Systems, Signals and Image Processing IWSSIP 1999*, pages 77–80, Bratislava, Slovakia, 2-4 Jun. 1999.
- [10] C. Vertan, M. Zamfir, E. Zaharescu, V. Buzuloiu, and C. Fernandez-Maloigne. Non-linear color image filtering by color to planare shape mapping. In *Proc. of ICIP 2003*, volume 2, pages 808–811, Barcelona, Spain, 10-13 Sept. 2003.
- [11] Z. Wang and A. C. Bovik. A universal image quality index. *IEEE Signal Processing Letters*, 9(3):81–84, 2002.